

## **High-Speed OTDM Demultiplexer based MZI, UNI**

البوابات المعتمدة على الاتصالات الضوئية متعددة الإرسال عالية السرعة

Dr. Ibrahim A.Murdas  
Electrical Engineering Dept.  
Babylon University

### **Abstract:**

Two types of semiconductor optical amplifier (SOA) – based optical gate are investigated, the Mach-Zender Interferometer (MZI), Ultra fast nonlinear interferometer (UNI). The gate are characterized by switch window calculation. The switching windows are evaluated using different criteria such as switching width and on-off contrast ratio to compare the performance of the gates. The results indicate clearly that, with a suitable parameters control, a switching window width of  $\approx 2$  ps and on-off contrast ratio below -11 dB can be achieved. The performance of the gates are investigated for demultiplexing application using the integrated contrast ratio (ICR). Simulation results are presented for OTDM bit rates up to 560 Gb/s and base data rate of 10Gb/s and 40Gb/s. the effect of SOA injection current ,control pulse energy and SOA length also presented.

### **المخلص:**

تم دراسة نوعين من البوابات MZI, UNI المعتمدة في عملها على المضخمات البصرية شبه الموصله . هذه البوابات تم تمييزها بواسطة عملية حساب نافذة المفاتيح . باستخدام معايير مختلفة مثل عرض نافذة المفتاح ونسبة التباين مابين الإطفاء والتشغيل حسب نوافذ المفاتيح لمقارنة أدائية البوابات . النتائج إشارة بشكل واضح إلى أن معلومات السيطرة الملائمة تكون مع عرض نافذه تقريبا 2 ps ونسبة تباين -11dB . أدائية هذه البوابات ك Demultiplexer في أنظمة OTDM تم مقارنتها بواسطة عملية حساب نسبة التباين المتكاملة (ICR). كما قدمت نتائج المحاكاة لـ OTDM لسرع تصل الى 560Gb/s وقاعدة بيانات 40Gb/s and 10Gb/s. كما تم تقديم تأثير كل من التيار المحقون وطاقة نبضة السيطرة وطول المضخمه شبه الموصله على نسبة التباين المتكامله (ICR).

## **I. INTRODUCTION**

High-Speed Optical telecommunication Network with terabit transmission capabilities can be achieved if the data remain in the optical format and bottlenecks due to the optical to electrical conversion are avoided. These systems required ultrafast signal processing like optical multiplier, add/drop functions ,optical demultiplexer and wavelength conversion [3]. Due to the high data rate, only all-optical switching method can be employed [7] . All-Optical switching involves the use of an optical control signal to switch data in the optical domain by taking advantage of the nonlinear effect that are presented in semiconductor devices. Since these nonlinear effect occur in time scale in the order of a few femto- seconds ( $10^{-15}$ ) [8]. They can be used for high speed switching Starting from SOA-based nonlinear interferometric structure and using optical nonlinearities in semiconductor material, various approach have been proposed and used for all-optical signal processing . using several interferometric configuration (e.g MZI,UNI, sagnac, etc) [5], all-optical demultiplexer for TDM data signal with line bit rate of up to 160Gb/s has been demonstrated [6]. In this work ,all-optical interferometric gate based on SOA are investigated as OTDM demultiplexer.

## **II .Switching Types**

### **A. Mach-Zehnder Interferometer(MZI)**

One of an interferometer gate is shown schematically in Figure 1. It consists of a nonlinear medium incorporated in an interferometer setup in this case MZI.

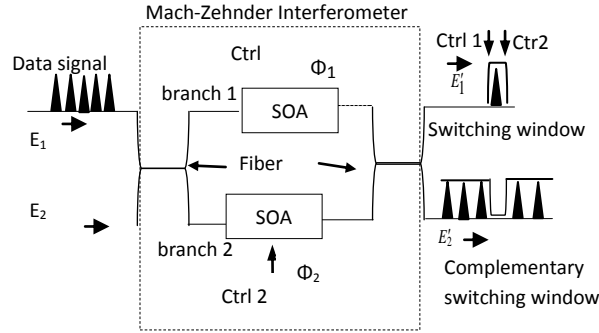


Figure1 Schematic of mach-zehnder interferometer switch based on SOAs as nonlinear medium.

In the Jones formulism [1] an optical systems, such as an interferometer, can be described by a transfer matrix (Jones matrix)  $M$  . That relates the output field to the input field  $E$

$$E' = ME \quad \text{--- (1)}$$

Where

$E = \begin{pmatrix} E_x \\ E_y \end{pmatrix}$  and  $E' = \begin{pmatrix} E'_x \\ E'_y \end{pmatrix}$  are four-dimensional vectors

$$\begin{bmatrix} E'_1 \\ E'_2 \end{bmatrix} = \begin{bmatrix} M_{11} & M_{12} \\ M_{21} & M_{22} \end{bmatrix} \begin{bmatrix} E_1 \\ E_2 \end{bmatrix} \quad \text{----(2)}$$

Equation (2) is written in a compact form. The Jones matrix of the MZI is denoted by MMZI whose elements  $M_{pq}$  ( $p, q \in 1, 2$ ) are given by

$$M_{11} = J_{(2)}^{bar} J_{(1)}^{(1)} J_{(1)}^{bar} + J_{(2)}^{cross} J_{(2)}^{(2)} J_{(1)}^{cross} \quad \text{--- (3)}$$

$$M_{12} = J_{(2)}^{cross} J_{(1)}^{(1)} J_{(1)}^{bar} + J_{(2)}^{bar} J_{(2)}^{(2)} J_{(1)}^{cross}$$

$$M_{21} = J_{(2)}^{bar} J_{(1)}^{(1)} J_{(1)}^{cross} + J_{(2)}^{cross} J_{(2)}^{(2)} J_{(1)}^{bar}$$

$$M_{22} = J_{(2)}^{cross} J_{(1)}^{(1)} J_{(1)}^{cross} + J_{(2)}^{bar} J_{(2)}^{(2)} J_{(1)}^{bar}$$

and

$$J_{(1)}^{bar} \quad J_{(2)}^{bar} \quad J_{(1)}^{cross} \quad J_{(2)}^{cross}$$

Are the Jones matrices for bar and cross coupling in the fiber couplers, and are given by [4] .

$$J_{(1)}^{bar} = \sqrt{1-k} \begin{bmatrix} \sqrt{1-k_x} & 0 \\ 0 & \sqrt{1-k_y} \end{bmatrix} \quad J_{(1)}^{cross} = \sqrt{1-k} \begin{bmatrix} j\sqrt{k_x} & 0 \\ 0 & j\sqrt{k_y} \end{bmatrix} \quad \text{-----(4)}$$

$J_{(2)}^{(1)} \quad J_{(2)}^{(2)}$  and optical paths characterization The power transmission coefficient ( $p, q \in \{1, 2\}$ )

$$T_{pq} |E_p|^2 = |M_{pq} E_p|^2 \quad \text{-----(5)}$$

The Jones matrices  $J^{(1)}$  and  $J^{(2)}$  for propagation through polarization sensitive SOAs in the upper and lower interferometer branches are given by

$$J^{(1)} = \begin{bmatrix} \sqrt{G_1(\Delta t)} e^{j\Phi_1(\Delta t)} & 0 \\ 0 & \sqrt{G_1(\Delta t)} e^{j\Phi_1(\Delta t)} \end{bmatrix} \quad J^{(2)} = \begin{bmatrix} \sqrt{G_1(\Delta t - \Delta \tau)} e^{j\Phi_1(\Delta t - \Delta \tau)} & 0 \\ 0 & \sqrt{G_1(\Delta t - \Delta \tau)} e^{j\Phi_1(\Delta t - \Delta \tau)} \end{bmatrix} \quad \text{---(6)}$$

where  $(\sqrt{G_2(\Delta t - \Delta \tau)})$  and  $\Phi_2(\Delta t - \Delta \tau)$  are the gain and phase for the data signal propagating through the SOA in the upper (lower) branch the transmission coefficient for the upper MZI output port ('demux port') is calculated by substituting equations (6) into (3) and using the transfer matrix  $M_{MZI}$  then equation (5)

$$T_{11}(E_{in}^* E_{in}) = (M_{11} E_{in})^* (M_{11} E_{in}) \quad \text{-----(7)}$$

$$\Rightarrow T_{11} = k^{(1)} k^{(2)} G(\Delta t - \Delta \tau) + (1 - k^{(1)})(1 - k^{(2)}) G(\Delta t)$$

$$- 2 \sqrt{k^{(1)} k^{(2)} (1 - k^{(1)})(1 - k^{(2)})} \sqrt{G(\Delta t - \Delta \tau) G(\Delta t)} \cos(\Delta \Phi(\Delta t))$$

The interferometer output power can be related to the nonlinear phase shift through the following relationship

$$P_{out}(\Delta t) = T_{11}(\Delta t) P_{in}$$

$$P_{out}(\Delta t) = k^{(1)} k^{(2)} G(\Delta t - \Delta \tau) P_{in} + (1 - k^{(1)})(1 - k^{(2)}) G(\Delta t) P_{in} - 2 \sqrt{k^{(1)} k^{(2)} (1 - k^{(1)})(1 - k^{(2)})} \sqrt{G(\Delta t - \Delta \tau) G(\Delta t)} \cos(\Delta \Phi(\Delta t)) P_{in} \quad \text{-----(8)}$$

## B. Ultrafast Nonlinear Interferometer (UNI)

The Ultrafast-Nonlinear Interferometer (UNI) is shown in Figure 2

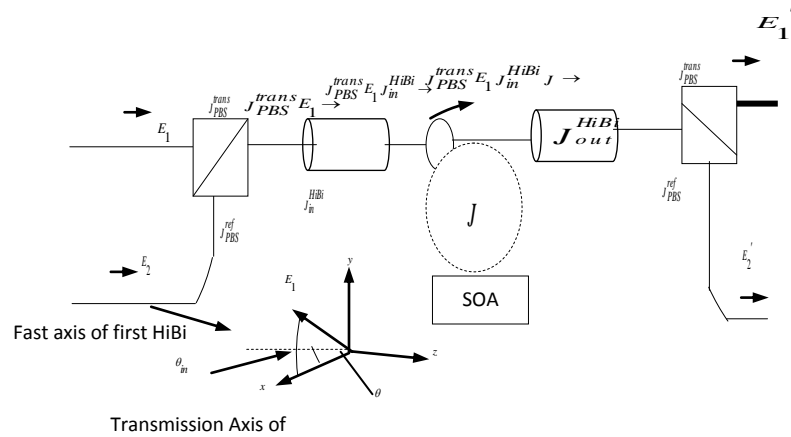


Figure 2 Schematic of ultrafast-nonlinear interferometer switch based on SOAs as nonlinear medium.

The waves at the UNI output can be written in the following compact form:

$$\begin{pmatrix} E_1' \\ E_2' \end{pmatrix} = \begin{pmatrix} M_{11} & M_{12} \\ M_{21} & M_{22} \end{pmatrix} \begin{pmatrix} E_1 \\ E_2 \end{pmatrix}$$

$M_{UNI}$

----(9)

where the components of the transfer matrix  $M_{UNI}$  are given by

$$\begin{aligned} M_{11} &= J_{PBS}^{trans} J_{out}^{HiBi} J J_{in}^{HiBi} J_{PBS}^{trans} & M_{12} &= J_{PBS}^{ref} J_{out}^{HiBi} J J_{in}^{HiBi} J_{PBS}^{trans} \\ M_{21} &= J_{PBS}^{trans} J_{out}^{HiBi} J J_{in}^{HiBi} J_{PBS}^{ref} & M_{22} &= J_{PBS}^{ref} J_{out}^{HiBi} J J_{in}^{HiBi} J_{PBS}^{ref} \end{aligned} \quad ----(10)$$

$$\begin{aligned} J_{PBS}^{trans} \text{ and } J_{PBS}^{ref} \\ J_{in}^{HiBi} = R(-\theta) \sqrt{1-k_{HiBi}} \begin{pmatrix} e^{j\Phi_{DGD}} & 0 \\ 0 & 1 \end{pmatrix} R(\theta) \quad J_{PBS}^{ref} = \begin{pmatrix} 0 & 0 \\ 0 & 1 \end{pmatrix} \quad J_{PBS}^{trans} = \begin{pmatrix} 1 & 0 \\ 0 & 0 \end{pmatrix} \end{aligned} \quad ----(11)$$

$$= \sqrt{1-k_{HiBi}} \begin{pmatrix} e^{j\Phi_{DGD} \cos^2(\theta) + \sin^2(\theta)} & (e^{j\Phi_{DGD}}) \cos(\theta) \sin(\theta) \\ (e^{j\Phi_{DGD}} - 1) \cos(\theta) \sin(\theta) & e^{j\Phi_{DGD}} \sin^2(\theta) \cos^2(\theta) \end{pmatrix} \quad ---(12)$$

$$\begin{aligned} J_{in}^{HiBi} &= J_{in}^{HiBi} \left( \theta + \frac{\pi}{2} \right) \\ &= \sqrt{1-k_{HiBi}} \begin{pmatrix} e^{j\Phi_{DGD} \sin^2(\theta) + \cos^2(\theta)} & -(e^{j\Phi_{DGD}}) \sin(\theta) \cos(\theta) \\ -(e^{j\Phi_{DGD}} - 1) \sin(\theta) \cos(\theta) & e^{j\Phi_{DGD}} \cos^2(\theta) \sin^2(\theta) \end{pmatrix} \end{aligned} \quad ----(13)$$

The Jones matrix  $J$ , describing the propagation of the split signals through the SOA, which is polarization sensitive, is given by

$$J = R(-\theta) \begin{pmatrix} \sqrt{G(\Delta t)} e^{j\Phi(\Delta t)} & 0 \\ 0 & \sqrt{G(\Delta t - \Delta \tau)} e^{j\Phi(\Delta t - \Delta \tau)} \end{pmatrix} R(\theta)$$

$$= \begin{bmatrix} \sqrt{G(\Delta t)} e^{j\Phi(\Delta t)} \sin^2(\theta) + \sqrt{G(\Delta t - \Delta \tau)} e^{j\Phi(\Delta t - \Delta \tau)} \cos^2(\theta) & [\sqrt{G(\Delta t)} e^{j\Phi(\Delta t)} - \sqrt{G(\Delta t - \Delta \tau)} e^{j\Phi(\Delta t - \Delta \tau)}] \sin(\theta) \cos(\theta) \\ [\sqrt{G(\Delta t)} e^{j\Phi(\Delta t)} - \sqrt{G(\Delta t - \Delta \tau)} e^{j\Phi(\Delta t - \Delta \tau)}] \sin(\theta) \cos(\theta) & \sqrt{G(\Delta t)} e^{j\Phi(\Delta t)} \cos^2(\theta) + \sqrt{G(\Delta t - \Delta \tau)} e^{j\Phi(\Delta t - \Delta \tau)} \sin^2(\theta) \end{bmatrix} \quad -----(14)$$

where  $(\theta)$  is the angle between the polarization of the leading data component in the SOA and the  $x$  axis[2].

### III. Switching Window

The switching windows are analyzed to extract the switching parameters related to ultrafast all-optical demultiplexing

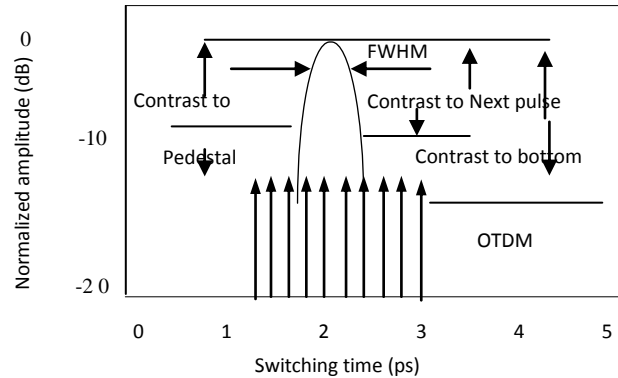


Figure 3 Parameters of the switching window.

To compare the performance of switching windows and to analyze the switching performance, some parameters have to be extracted. These parameters describe the width and the depth of the switching window. The width of the switching window can be expressed by the full width at half maximum (FWHM). Depending on the bit rate of the data stream, there is a maximum width which can be tolerated for a successful switching performance. The maximum width is equal to the bit period of the data signal. If the FWHM is larger than this maximum, adjacent OTDM channels will be also switched. The minimum width of the switching window depends on the pulse width of data signal, the window width and the on-off contrast ratio. These quantities are not always sufficient to characterize signal stream performance for different type switch. An integrative approach for the definition of the switching contrast is therefore reasonable. The ICR is designed to evaluate the performance of the switch as demultiplexer in an OTDM system.

## IV. Comparison of Switching

### A. 10Gb/s Base data rate

The values are calculated for line data rate 40, 160, and 320 Gb/s as a function of a switching window as shown in Figure 4. The curves for all switching have a similar shape for small window widths. The ICR decrease, independent of the TDM bit rate, because the switching window collapse. For large window width, the ICR decrease when the switching window becomes broader than the data bit period.

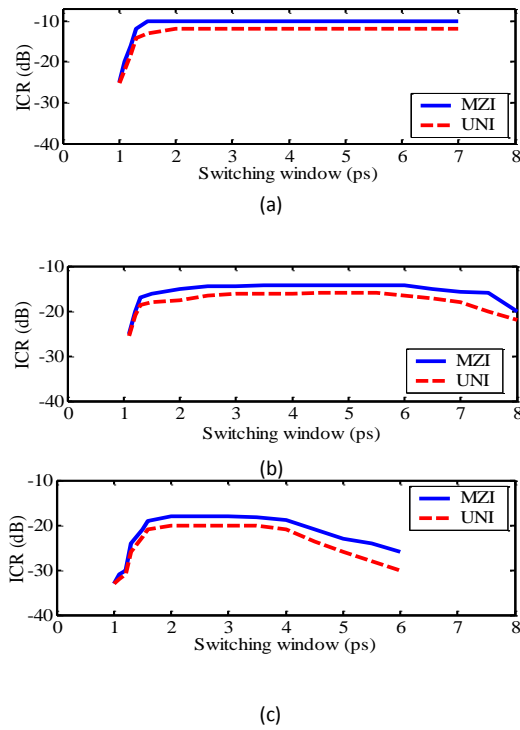


Figure 4 ICR-Window width characteristic for MZI and UNI –based OTDM demultiplexer at 10GHz control pulse rate and line rate(a) 40Gbit/s (b) 160Gbit/s (c) 320 Gbit/s.

## B. 40Gb/s Base data rate

The influence of the higher base data rate 40Gb/s on the ICR is shown in Figure 5 for MZI , UNI switch . in this figure the ICR calculated for data rate 160,320,540Gb/s.

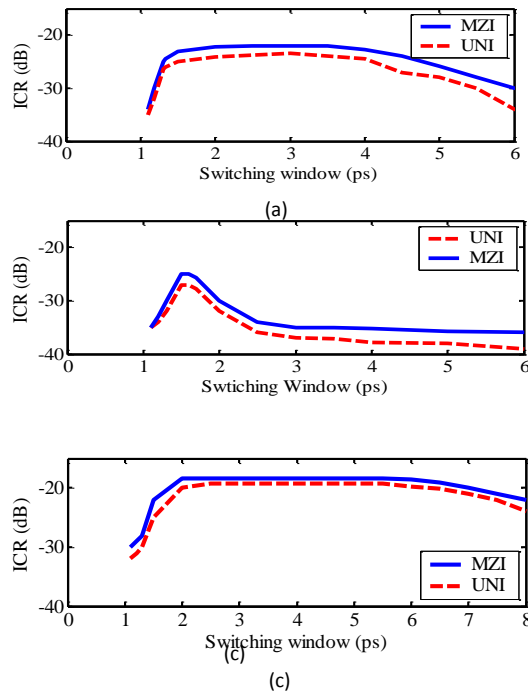


Figure 5 ICR values for MZI and UNI switches for demultiplexing from a line bit rate of a) 160 Gbit/s, b) 320 Gbit/s and c) 540 Gbit/s to 40 Gbit/s base data rate.

The point at which the crosstalk leads to a decrease in ICR depends on the data bit period and switching window. For 160 Gbit/s, the decrease is slow and starts around 6 ps. For 320 Gbit/s the decrease is significantly faster and starts at about 4 ps. This is also true for higher data rate; at 600 Gb/s the decrease began at 2 ps. For both UNI and the MZI, the ICR values are well above -35 dB for 540 Gbit/s.

## **V) Results**

### **A ) Effect of SOA injection current**

The influence of SOA driving current on the ICR at 10Gb/s base data rate was shown in Figure 6 for MZI and UNI switches. The values of ICR for the MZI are -15, -14, and -14.8 dB at 0, 200, and 300 mA, respectively. This is mainly due to the lower phase shift observed in the direct phase calculations. These values are to be compared with -17, -16 and -16.7 for UNI.

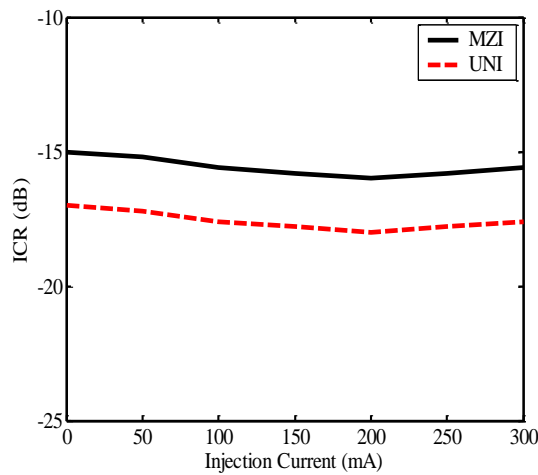


Figure 6 shows the ICR as a function of the injection current.

The results are about 1.8 ps, 2ps for MZI and UNI switches respectively, for SOA driving current of 0 mA.

### **B. Effect of Control pulse power**

The ICR increases strongly with increase control pulse energy as shown in Figure 7. ICR= -12dB for control pulse energy of 3.5 pJ, this is mainly due to the higher phase shift observed in the direct phase calculations.

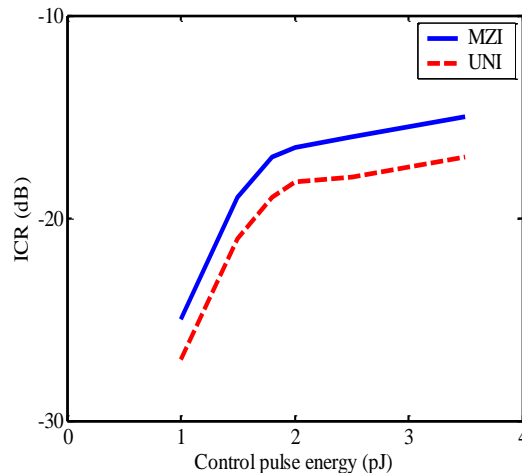


Figure 7 shows the ICR as a function of the control pulse energy.

### C) Effect of SOA length on ICR

The influence of the SOA length on the ICR is shown in Figures 8 a, b and c for the MZI and the UNI switches. In these figure, the ICR for 160 Gb/s demultiplexer is calculated at 40 Gb/s base data rate and plotted as function of the switching window width. The results indicate that  $L=1.55$  mm gives the highest values of ICR.

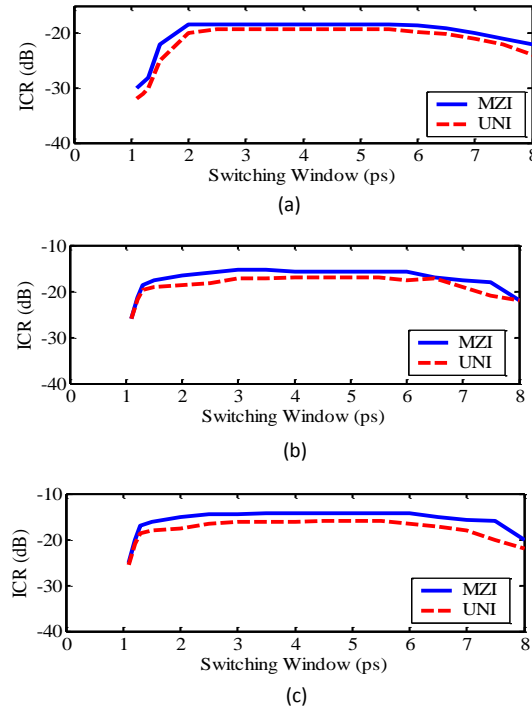


Figure 8 ICR versus s witching window for different SOA length a)  $L=0.75$  mm b)  $L=1$  mm c)  $L=1.55$  mm

### D .Effect of TPA on ICR

The effect of TPA on the ICR is shown in Figure 9 a and b where the lower ICR is obtained when removing the TPA factor. This reduction is due to the decrease of the output power of the interferometer. This decrease occurs because this power depends on the nonlinear phase shift of the interferometer Figure 9b shows that lower phase shift is obtained when removing TPA factor.

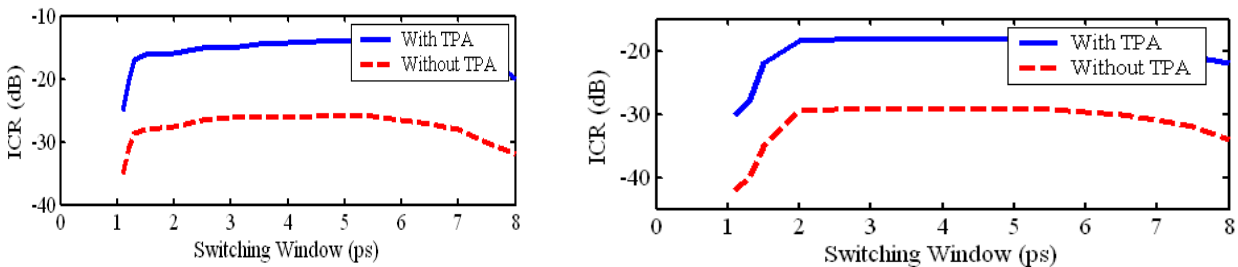


Figure 9 ICR for CH at line data rate 160 Gb/s and base data rate a) 10Gb/s b) 40Gb/s.



## **VI) Conclusion**

Switching window calculation has been performed on two types of all-optical interferometric switches, based on XPM in SOAs. The ICR calculation has been introduced to evaluate the numerical experimental switching windows and discuss the demultiplexing capabilities of the switches in an OTDM system.

Comparing the demultiplexing capabilities of both switches reveals the following conclusions For the MZI switch, switching windows as short as 2 ps (FWHM) and ICR values well above -15 dB are achieved at line rates of 160 Gb/s and base data rate 10Gb/s. The UNI switch has somewhat lower ICR values, about 2.5 dB and the shortest possible switching window is about 2.2 ps (FWHM). The predicted ICR values reveals that the UNI switch shows a considerably lower demultiplexing performance compared to the MZI Switched. The values of ICR are reduced by 9dB when the model takes into account CH effect and neglects the TPA effect. The highest ICR is obtained at 40 Gb/s base data rate with  $L=1.55$  mm SOA length where maximum nonlinear phase shift is obtained. The ICR is a good measure to compare different types of optical switches and to estimate their demultiplexing capabilities, far better than the widely used normal contrast definitions.

## **References**

1. A. Yariv, 1997 "Optical Electronic in Modern communication" Oxford University Press, Inc. New York.
2. C. Bintjas, K. Vlachos, 2003 "Ultrafast Nonlinear Interferometer (UNI)-Based Digital Optical Circuits and Their Use in Packet Switching" Journal of Light wave technology, **21**, PP. 2629-2631.
3. G. Giuliani, S. Donati, 2005 "Simulation of all-optical demultiplexing utilizing Two-Photon Absorption in Semiconductor devices for High-Speed OTDM network" IEEE Photonics Technology letter, **16**, PP. 990-992.
4. J. Van der Tol, 2001 "A Mach-Zehnder-Interferometer-Based Low-Loss Combiner" IEEE Photonics Technology Letters, **13**, PP. 1197-1199.
5. R. Schrieck, M. Kwakernaak, 2001 "Ultrafast Switching Dynamics of Mach-Zehnder Interferometer Switches" IEEE Photonics Technology Letters, **13**, PP. 603-605.
6. R. Ngah, Z. Ghassemlooy, and G. Swift, 2002 "Simulation of an All Optical Time Division Multiplexing Router Employing Symmetric Mach-Zehnder (SMZ)". HFPSC2002, PP. 130-136.
7. S. Hamilton, B. Robinson, and T. Murphy, 2002 "100 Gb/s optical time-divisions multiplexed networks" Lightwave Technology, **20**, PP. 2086-2100.
8. Y. Ueno, S. Nakamura and K. Tajima, 2001 "Nonlinear phase shifts induced by semiconductor optical amplifiers with control pulses at repetition frequencies in the 40-160-GHz range for use in ultrahigh-speed all-optical signal processing", Journal of Optical Society American B, **19**, PP. 2573-2589.